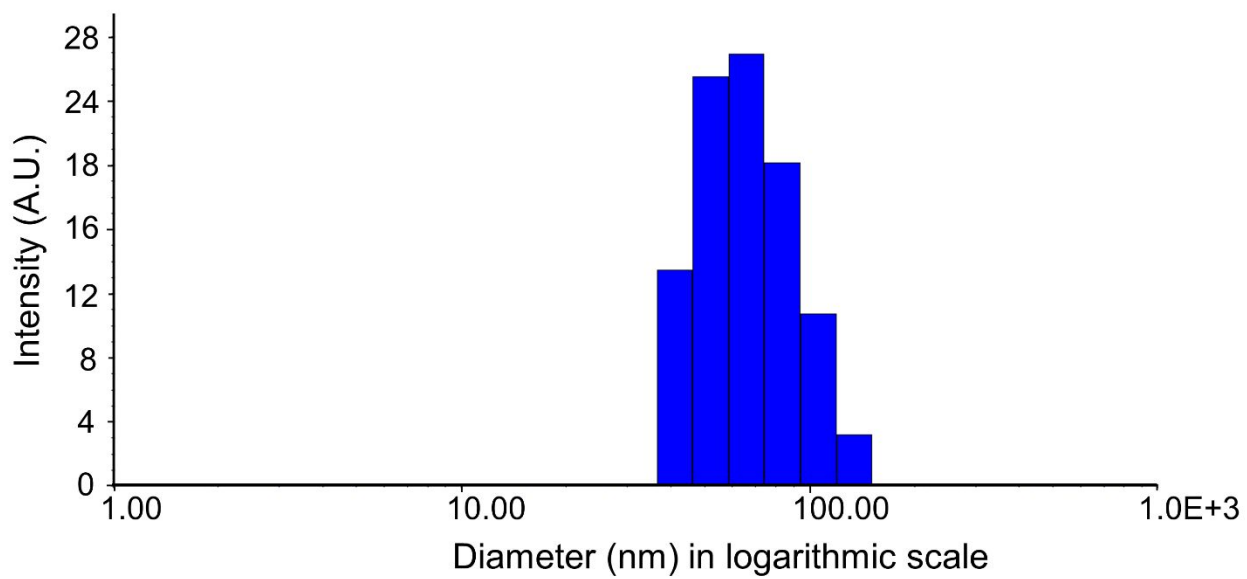


# Supporting Information

## Untwisted $\alpha$ -synuclein Filaments formed in the Presence of Lipid Vesicles

Anvesh K. R. Dasari<sup>1</sup>, Lucas Dillard<sup>2</sup>, Sujung Yi<sup>1</sup>, Elizabeth Viverette<sup>2</sup>, Alimohammad Hojjatian<sup>3</sup>, Urmi Sengupta<sup>4</sup>, Rakez Kayed<sup>4</sup>, Kenneth A. Taylor<sup>3</sup>, Mario Juan Borgnia<sup>2</sup>, Kwang Hun Lim<sup>1,\*</sup>

<sup>1</sup>Department of Chemistry, East Carolina University, Greenville, NC 27858, USA. <sup>2</sup>Genome Integrity and Structural Biology Laboratory, National Institute of Environmental Health Sciences, National Institutes of Health, Department of Health and Human Services, Research Triangle Park, NC, 27709, USA. <sup>3</sup>Institute of Molecular Biophysics, Florida State University, Tallahassee, FL 32306-4380, USA. <sup>4</sup>Departments of Neurology, Neuroscience and Cell Biology, University of Texas Medical Branch, Galveston, TX, 77555, USA.



**Figure S1:** Size distribution chart of DMPS lipid vesicles measured by DLS at a laser wavelength of 658 nm.

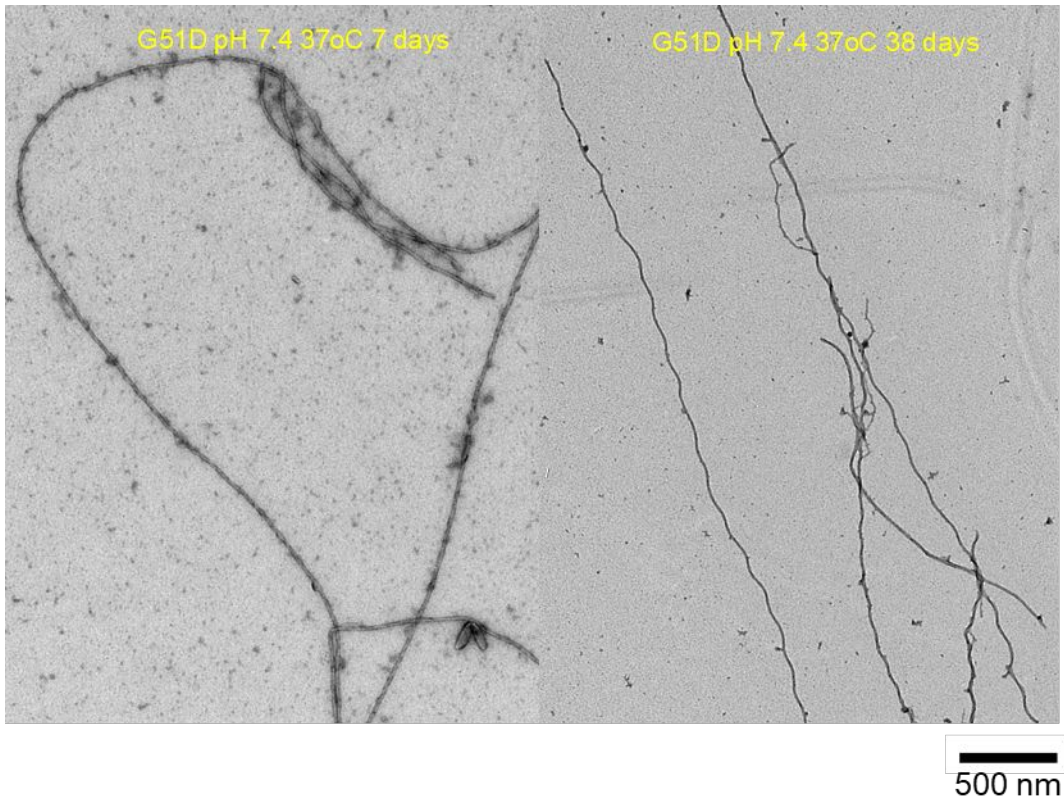


**Figure S2.** TEM images of G51D  $\alpha$ -synuclein filaments formed in the presence of DMPS (100  $\mu\text{M}$ ) vesicles with a diameter of 70 nm at pH 7.4.

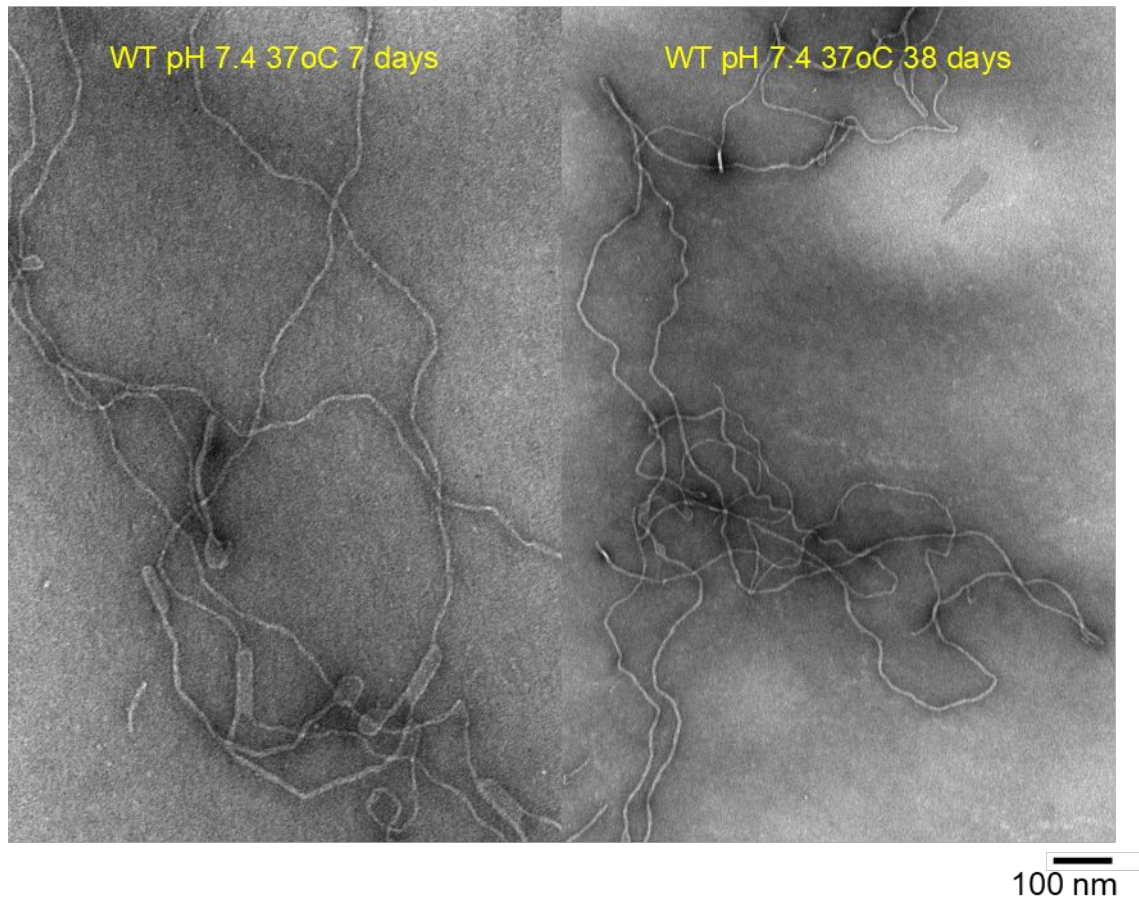


**Figure S3.** TEM images of WT  $\alpha$ -synuclein filaments formed in the presence of DMPS (100  $\mu$ M) vesicles with a diameter of 70 nm at pH 7.4.

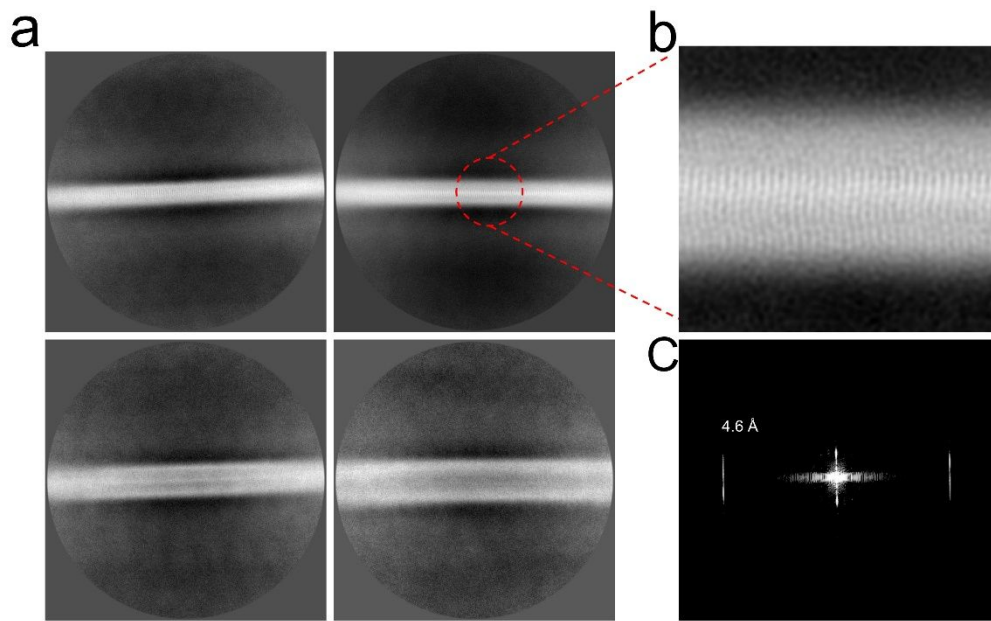


**Figure S4.** (A) Reference-free 2D class averages of  $\alpha$ -synuclein filaments formed in the presence of DMPS SUVs obtained at a larger box size of 74 nm showing no observable twist. (B) Magnified image of a 2D class average showing the inter-strand spacing of 4.6 Å in  $\alpha$ -synuclein fibrils. (C) Representative power spectrum of a reference-free 2D class average.

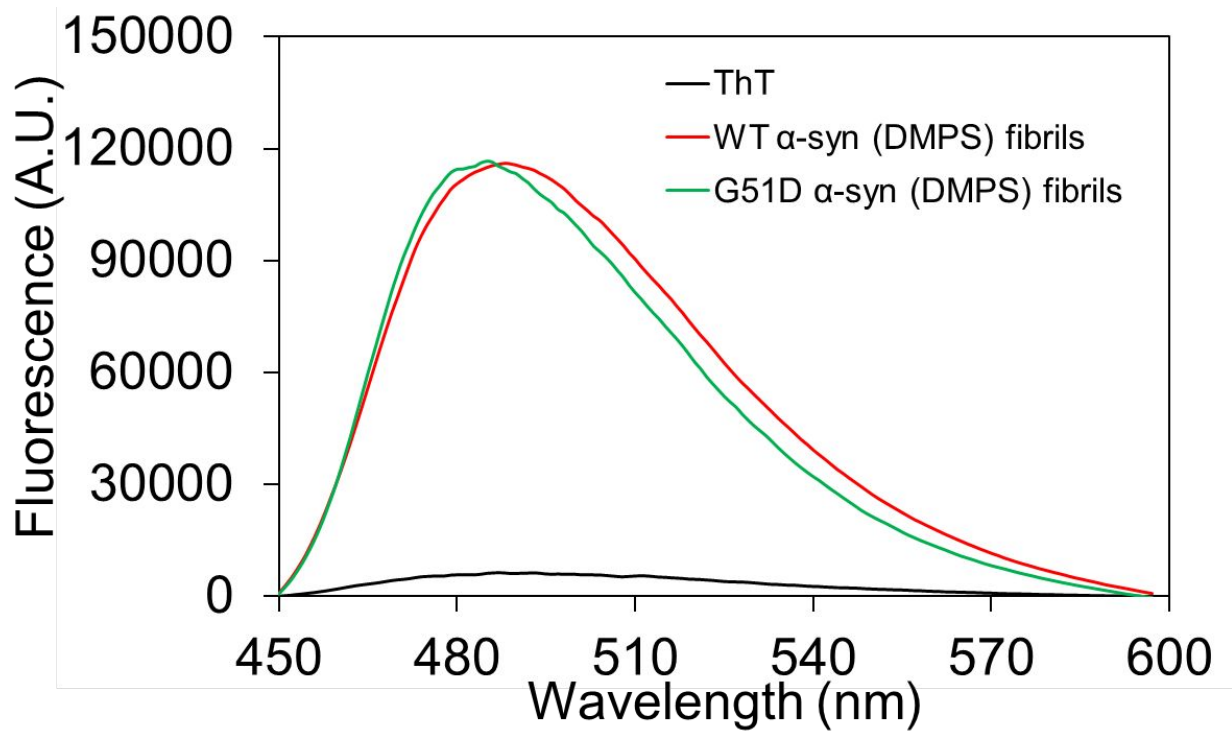


**Figure S5.** ThT fluorescence of DMPS-derived  $\alpha$ -synuclein filaments. The DMPS-derived  $\alpha$ -synuclein filaments (5  $\mu$ M) were mixed with ThT working solution (50  $\mu$ M), and the ThT fluorescence was measured with an excitation wavelength of 440 nm.

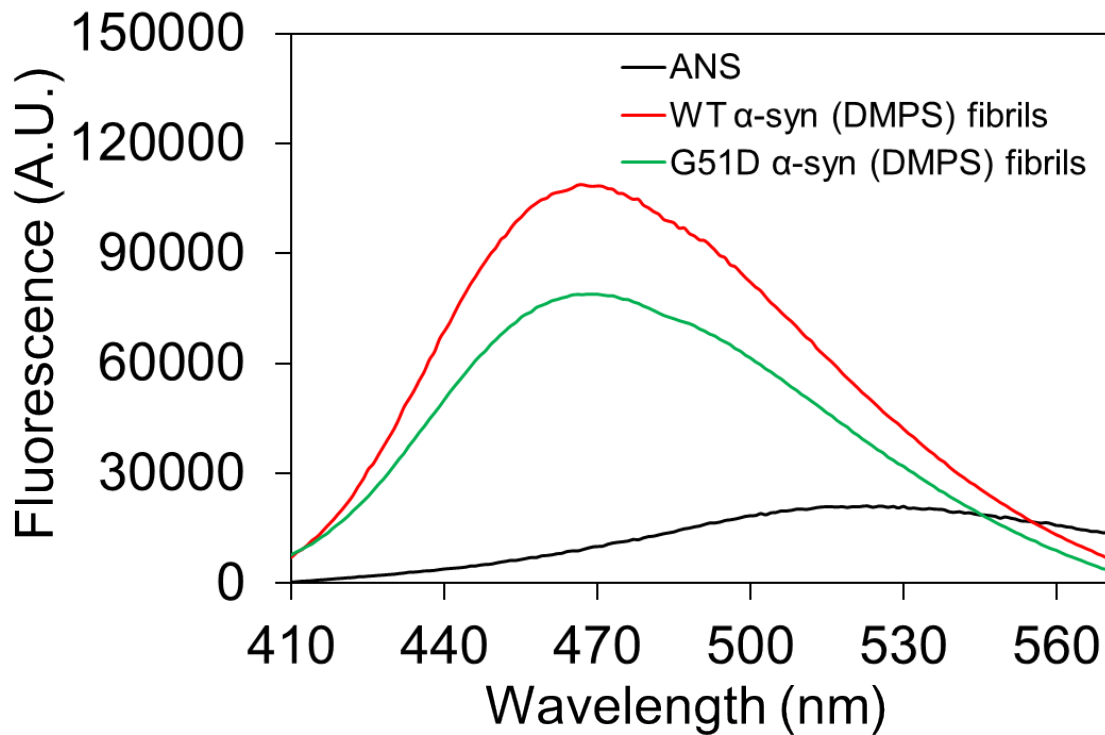


**Figure S6.** ANS fluorescence of the DMPS-derived  $\alpha$ -synuclein filaments. The fluorescence was monitored at an excitation wavelength of 350 nm for the filamentous aggregates (5  $\mu$ M) in the presence ANS (20  $\mu$ M) with an excitation wavelength of 350 nm. A previous study showed that ANS binds fibrillar aggregates through electrostatic interactions between the dye molecule and sidechains of the basic amino acids.<sup>1</sup> The single-point mutation (G51D) on the positively charged N-terminal region of  $\alpha$ -synuclein may partly inhibit the ANS binding, resulting in the slightly reduced fluorescence intensity for the DMPS-derived G51D  $\alpha$ -synuclein filament.

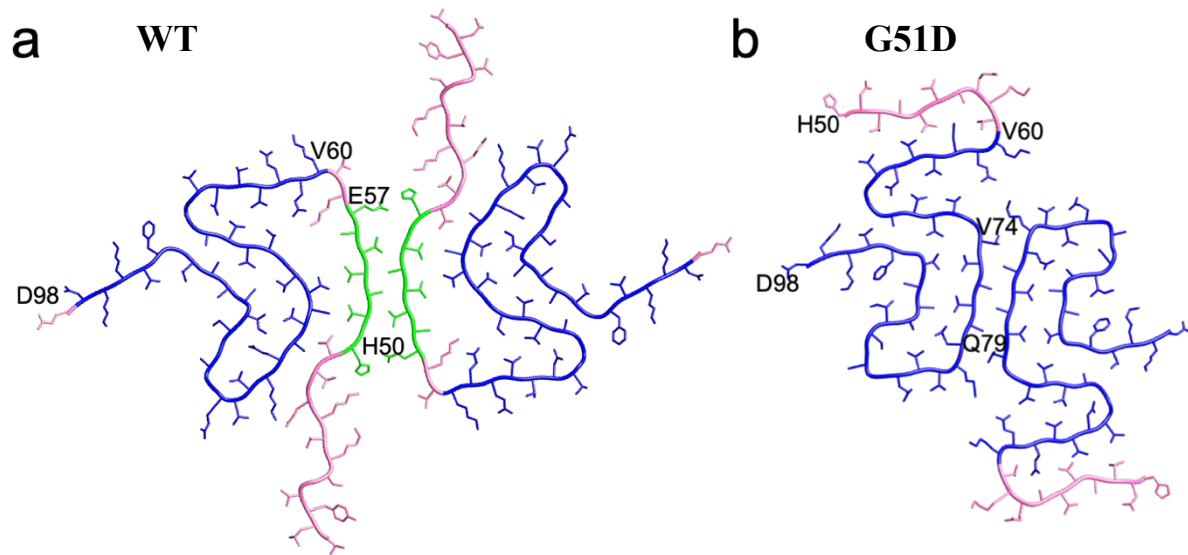


**Figure S7.** Cryo-EM structures of WT (a) and G51D (b)  $\alpha$ -synuclein fibrils formed in the absence of DMPS. Cryo-EM structures revealed that both WT and G51D  $\alpha$ -synuclein fibrils contain a similar fibril core region (V60 - D98, shown in blue).<sup>2,3</sup> The interfacial region (H50 – E57) in the WT  $\alpha$ -synuclein fibrils is shown in green. The cryo-EM structures of the WT and G51D fibrils formed in the absence of DMPS are adapted from the references 2 and 3.

|                  |                  |                  |
|------------------|------------------|------------------|
| 5.4 nm<br>(724)  | 6.7 nm<br>(1969) | 7.6 nm<br>(769)  |
| 7.6 nm<br>(2625) | 9.1 nm<br>(1114) | 13.0 nm<br>(643) |

**Table S1.** The thicknesses (in nm) of  $\alpha$ -synuclein filaments for each 2D class average. The reference-free 2D class averages were obtained using a box size of 56 nm (Figure 4). The number of particles for each 2D class average is enclosed in parenthesis.

| PDB ID | Half-pitch (nm) |
|--------|-----------------|
| 6A6B   | 120             |
| 6OSJ   | 121             |
| 6CU7   | 92              |
| 6SSX   | 108             |
| 6SST   | 96              |
| 7L7H   | 63              |
| 6XYO   | 80              |
| 6XYP   | 80              |
| 7NCA   | 80              |
| 7NCG   | 90              |

**Table S2.** Helical twists of various previously reported polymorphs of  $\alpha$ -synuclein. polymorphs 1a (6a6b, 6osj, 6cu7)<sup>4,5</sup>, polymorph 2a (6ssx)<sup>6</sup>, polymorph 2b (6sst)<sup>6</sup>, tau-promoted polymorph (7l7h)<sup>7</sup>, MSA type 1 (6XYO)<sup>8</sup>, MSA type 2 (6XYP)<sup>8</sup>, MSA seeded type 1a (7NCA)<sup>9</sup>, and type 2a (7NCG)<sup>9</sup>.

|                                     | $\alpha$ -Helix (%) | $\beta$ -Sheet (%) | Disordered (%) |
|-------------------------------------|---------------------|--------------------|----------------|
| WT $\alpha$ -syn fibrils            | 10                  | 34                 | 56             |
| G51D $\alpha$ -syn fibrils          | 13                  | 33                 | 54             |
| WT $\alpha$ -syn (DMPS) filaments   | 27                  | 24                 | 49             |
| G51D $\alpha$ -syn (DMPS) filaments | 26                  | 25                 | 49             |

**Table S3.** Secondary structural analyses of WT and G51D  $\alpha$ -synuclein filaments formed in the presence and absence of DMPS using DichroWeb<sup>10</sup>.

## References

1. Sulatsky, M. I., Sulatskaya, A. I., Povarova, O. I., Antifeeva, I. A., Kuznetsova, I. M., and Turoverov, K. K. (2020) Effect of the fluorescent probes ThT and ANS on the mature amyloid fibrils. *Prion*, 14, 67-75.
2. Li, B., Ge, P., Murray, K. A., Sheth, P., Zhang, M., Nair, G., Sawaya, M. R., Shin, W. S., Boyer, D. R., Ye, S., Eisenberg, D. S., Zhou, Z. H., and Jiang, L. (2018) Cryo-EM of full-length alpha-synuclein reveals fibril polymorphs with a common structural kernel. *Nat. Commun.* 9, 3609-2.
3. Sun, Y., Long, H., Xia, W., Wang, K., Zhang, X., Sun, B., Cao, Q., Zhang, Y., Dai, B., Li, D., and Liu, C. (2021) The hereditary mutation G51D unlocks a distinct fibril strain transmissible to wild-type  $\alpha$ -synuclein. *Nat. Commun.* 12, 6252-2.
4. Li, Y., Zhao, C., Luo, F., Liu, Z., Gui, X., Luo, Z., Zhang, X., Li, D., Liu, C., and Li, X. (2018) Amyloid fibril structure of alpha-synuclein determined by cryo-electron microscopy. *Cell Res.* 28, 897-903.
5. Li, B., Ge, P., Murray, K. A., Sheth, P., Zhang, M., Nair, G., Sawaya, M. R., Shin, W. S., Boyer, D. R., Ye, S., Eisenberg, D. S., Zhou, Z. H., and Jiang, L. (2018) Cryo-EM of full-length alpha-synuclein reveals fibril polymorphs with a common structural kernel. *Nat. Commun.* 9, 3609-2.
6. Guerrero-Ferreira, R., Taylor, N. M., Arteni, A. A., Kumari, P., Mona, D., Ringler, P., Britschgi, M., Lauer, M. E., Makky, A., Verasdonck, J., Riek, R., Melki, R., Meier, B. H., Bockmann, A., Bousset, L., and Stahlberg, H. (2019) Two new polymorphic structures of human full-length alpha-synuclein fibrils solved by cryo-electron microscopy. *eLife*. 8, 10.7554/eLife.48907.
7. Hojjatian, A., Anvesh K.R. D., Urmī S., Dianne T., Nadia D., Fatemeh A. Y., Lucas D., Brian M., Robert G. G., Mario J. B., Rakez K., Kenneth A. T., and Kwang H. L. (2021) Tau Induces Formation of  $\alpha$ -synuclein Filaments with Distinct Molecular Conformations. *Biochemical and Biophysical Research Communications*, 554, 145-50.

8. Schweighauser, M., Shi, Y., Tarutani, A., Kametani, F., Murzin, A. G., Ghetti, B., Matsubara, T., Tomita, T., Ando, T., Hasegawa, K., Murayama, S., Yoshida, M., Hasegawa, M., Scheres, S. H. W., and Goedert, M. (2020) Structures of alpha-synuclein filaments from multiple system atrophy. *Nature*, 585, 464-469.
9. Lövestam, S., Schweighauser, M., Matsubara, T., Murayama, S., Tomita, T., Ando, T., Hasegawa, K., Yoshida, M., Tarutani, A., Hasegawa, M., Goedert, M., & Scheres, S. (2021) Seeded assembly in vitro does not replicate the structures of  $\alpha$ -synuclein filaments from multiple system atrophy. *FEBS open bio*, 11(4), 999–1013.
10. Whitmore, L. and Wallace, B.A. (2004) DICHROWEB: an online server for protein secondary structure analyses from circular dichroism spectroscopic data. *Nucleic Acids Res*, 32, W668 - 73.